# Dual-Band Reduced-Order Model of an HVDC Link Embedded into a Power Network for EMT Studies

Ruiz, Carlos; Medina, Edgar; Ramirez, Abner; Mehrizi-Sani, Ali; Chavez Muro, Jose de Jesus; Davoudi, Ali; Abdel-rahman, Mohamed

**DOI**
10.1109/TEC.2019.2935892

**Publication date**
2019

**Document Version**
Final published version

**Published in**
IEEE Transactions on Energy Conversion

**Citation (APA)**
Ruiz, C., Medina, E., Ramirez, A., Mehrizi-Sani, A., Chavez Muro, J. D. J., Davoudi, A., & Abdel-rahman, M. (2019). Dual-Band Reduced-Order Model of an HVDC Link Embedded into a Power Network for EMT Studies. *IEEE Transactions on Energy Conversion*, *35 (2020)*(1), 416-424. Article 8805118. https://doi.org/10.1109/TEC.2019.2935892

# Dual-Band Reduced-Order Model of an HVDC Link Embedded Into a Power Network for EMT Studies

Carlos A. Ruiz-Zea, *Student Member, IEEE*, Edgar Medina, *Student Member, IEEE*, Abner Ramirez, *Senior Member, IEEE*, Ali Mehrizi-Sani, *Senior Member, IEEE*, Jose de Jesus Chavez, *Member, IEEE*, Ali Davoudi, *Senior Member, IEEE*, and Mohamed Abdel-Rahman, *Senior Member, IEEE*

***Abstract*—This paper presents an approach to obtain reduced-order models for power networks involving power electronic converters (PEC) via the frequency-domain balanced realizations (FDBR) technique. PECs play an essential role in power processing and energy conversion in modern electrical networks, such as the interconnection of renewable generators, HVDC links, and active filters. Integration of PECs into dynamic equivalents needs model-order reduction (MOR) in both low- and high-frequency ranges to account for both slow and fast dynamics due to the network and switching natures. The objective of the FDBR technique is to obtain an internally balanced system, i.e., an equally controllable/observable system, that can be reduced according to its *dominant* dynamics within the limited frequency bandwidths. This allows accounting for specific band-limited phenomena, such as those generated within a power network caused by PECs, which is the focus of this paper. The results show that faster yet accurate simulations are achieved by reduced-order models through FDBR compared to their full-order counterparts.**

***Index Terms*—Electromagnetic transient analysis, frequency-domain analysis, reduced order systems.**

## I. Introduction

A DETAILED representation of modern electrical power systems for electromagnetic transient (EMT) studies requires considerable computational resources [1]. This computational burden has been traditionally addressed by utilizing average value models (AVM), mainly accounting for DC and fundamental frequency, speeding up simulations at the cost of ignoring high-frequency dynamics [2]. Alternatively, MOR techniques aim to derive a reduced-order dynamic model that reproduces the most important dynamic properties of the original system. The reduced-order dynamic model diminishes computational complexity and utilizes less computational resources compared to the original system [1], [3]–[5]. Due to the damping effect and low-pass feature of linear power system components, transient phenomena do not travel far into the network, which is the traditional key motivation for reducing the size of large networks. MOR is applied in several fields, such as system identification, control, filtering, thermal models, hybrid electric vehicles, and power systems [6]–[8].

The main techniques utilized to reduce the model order in power systems can be broadly classified as:

- Modal analysis (MA).
- Singular value decomposition (SVD), which includes the classical time-domain balanced realization (BR) method.
- Moment matching (MM), also known as Krylov methods.

The above-mentioned techniques provide a reduced-order system in the form of a first-order state space representation [9], [10].

MOR techniques based on MA identify and preserve the dominants modes; however, the input and output characteristics are not completely preserved [11]. SVD-based methods, e.g., BR, characterize equally controllable and observable modes via Hankel singular values. Lyapunov equations are solved to calculate the system's Hankel values; such solution can imply computational burden for very large systems [10]. The MM methods are the most computationally efficient; however, they do not exhibit global error limits as in BR technique. Also, MM methods require selection of interpolation points, which is not automated and depends on the user's specifications.

In [12], an extended Krylov subspaces method is applied to reduce a large-scale power system in the low-frequency range, and then the reduced-order model is incorporated into an unstable power system to tune a PSS stabilizer. Also, with focus in the low-frequency range, [13] presents a novel model order reduction scheme for power networks based on clusters on which the structure of the network is preserved. A few applications of the classical BR technique, such as medium-voltage system and networks including wind power plants, are described in [14]. In [15], the model coherency method is combined with classical BR to produce reduced-order models of dynamic equivalents. In [16] linear modal analysis and proper orthogonal decomposition are combined to obtain reduced-order models for the analysis and control of inter-area oscillations.

Manuscript received April 6, 2019; revised July 3, 2019; accepted August 12, 2019. Date of publication August 19, 2019; date of current version February 19, 2020. Paper no. TEC-00376-2019. *(Corresponding author: Abner Ramirez.)*

C. A. Ruiz-Zea, E. Medina, and A. Ramirez are with CINVESTAV-Guadalajara, Zapopan 45019, Mexico (e-mail: caruiz@gdl.cinvestav.mx; eymedina@gdl.cinvestav.mx; abner.ramirez@cinvestav.mx).

A. Mehrizi-Sani was with Washington State University, Pullman, WA 99164 USA. He is now with Virginia Tech, Blacksburg, VA 24061 USA (e-mail: mehrizi@eecs.wsu.edu).

J. de J. Chavez is with Delft University of Technology, Delft 2628, CD, The Netherlands (e-mail: j.j.chavezmuro@tudelft.nl).

A. Davoudi is with the University of Texas at Arlington, Arlington, TX 76019 USA (e-mail: davoudi@uta.edu).

M. Abdel-Rahman is with Ain Shams University, Cairo 11566, Egypt (e-mail: mohamed_a_rahaman@eng.asu.edu.eg).

Color versions of one or more of the figures in this article are available online at http://ieeexplore.ieee.org.

Digital Object Identifier 10.1109/TEC.2019.2935892

Different MOR techniques have been applied to electrical systems involving PECs. In [17], classical BR is applied to a grid involving voltage source inverters (VSI). The grid is modeled as an infinite bus with an impedance in series; however, this representation is not able to accurately provide network dynamics. These dynamics play an important role in stability studies and must be considered to generate precise models leading to realistic scenarios [18].

Due to the presence of PECs in a power network, high frequencies must be considered to accurately represent switching frequencies. This justifies reducing the linear part of the network under analysis in both low- and high-frequency ranges. The inspiration for this research came from the fact that decreasing model order for a wide frequency range still accounts for an extensive range of dynamics whilst in some cases dynamics can be enclosed to the type of devices involved in the power network.

In this paper a balanced realization method in frequency-domain is used. BR is a mature and classic method that exhibits important guaranteed properties such as bounded approximation error [1], [5]. This procedure is based on the analysis of principal components of the impulse response of the system and relies on coordinate transformation of the original dynamic system to obtain an internally balanced system. This coordinate transformation is determined by equating the system's controllability and observability Gramians to a diagonal matrix containing the Hankel singular values, also known as the second-order modes of the system. The Hankel singular values provide a measure of the level of controllability/observability of the system allowing direct truncation to yield a stable reduced-order subsystem. More recently, BR has been structured in frequency-domain (FDBR) to reduce a system within a specific frequency range [19]. This paper expands the application of the FDBR technique to power systems simulations involving PECs and proposes a two-frequency band methodology to obtain the reduced-order model of power networks involving PECs via FDBR. The low-frequency (in the Hz range) and the high-frequency (in the kHz range) band approximations permit to simultaneously include slower dynamics, characteristic of the power network, and switching frequency dynamics, corresponding to PECs. This localized reduced-order model fitting represents computational savings compared to a reduced-order full-frequency range fitted system while preserving accuracy. The fact that alternative energy resources play an important role in modern power networks makes the proposed methodology applicable to cases where the power systems engineer desires to analyze the interfacing of PECs with a traditional network for EMT studies, especially nearby switching frequencies of PECs, as illustrated by the HVDC link case study presented in the paper. The methodology is applied to a power network involving an HVDC link and its application to other networks involving PECs is straightforward as long as the modeling differential/algebraic equations of the electronic part are available.

The basic theory of FDBR is presented in Section II. The proposed methodology is outlined in Section III. Numerical results are presented in Section IV. Analysis of approximation and time-domain simulation errors are further analyzed in Section V. Finally, Section VI concludes the paper.

## II. Fundamentals of FDBR

### A. FDBR Fundamental Theory

This section outlines the basic theory of FDBR [19]. The classical time-domain BR equations [5] are given in Appendix A. The presented theory is applicable to both single-input single-output (SISO) and multi-input multi-output (MIMO) systems.

Consider the *n*th order linear time-invariant (LTI) system given in (1), which represents the full-order system as characterized by parameters ($A$, $B$, $C$, $D$).

$$\begin{aligned} \dot{x} &= Ax + Bu \\ y &= Cx + Du \end{aligned} \tag{1}$$

Model order reduction is aimed at obtaining the *r*th order system $(A_r, B_r, C_r, D)$, as given in (2), with $r < n$, that closely reproduces the dynamics of the original full-order system (1) within the frequency range $[\Omega_1, \Omega_2]$.

$$\begin{aligned} \dot{x}_r &= A_r x_r + B_r u \\ y &= C_r x_r + Du \end{aligned} \tag{2}$$

The controllability $(W_{cf})$ and observability $(W_{of})$ Gramians of system (1) in the frequency range $[0, \Omega]$ are given by [1]

$$\begin{aligned} W_{cf} &= \frac{1}{2\pi}\int_{-\Omega}^{\Omega} (j\omega I - A)^{-1} BB^* (-j\omega I - A^*)^{-1} d\omega \\ W_{of} &= \frac{1}{2\pi}\int_{-\Omega}^{\Omega} (-j\omega I - A^*)^{-1} C^* C (j\omega I - A)^{-1} d\omega, \end{aligned} \tag{3}$$

where superscript $*$ denotes complex conjugate transpose and $I$ represents an $n \times n$ identity matrix. If the frequency range is changed to $[0, \infty]$, the classical controllability and observability Gramians are obtained [1]. Both Gramians in (3) satisfy the Lyapunov relations:

$$AW_{cf} + W_{cf}A^* = -(BB^*F^* + FBB^*), \tag{4a}$$

$$A^*W_{of} + W_{of}A = -(C^*CF + F^*C^*C), \tag{4b}$$

where:

$$F = \int_{-\Omega}^{\Omega} (j\omega I - A)^{-1} d\omega \tag{5}$$

Note that, once $F$ in (5) is calculated for the defined frequency range (see Appendix B), (4) is resolved for both Gramians. If the frequency range under interest is $[\Omega_1, \Omega_2]$, we compute the Gramians as follows:

$$\begin{aligned} W_{cf}(\Omega_1, \Omega_2) &= W_{cf}(\Omega_2) - W_{cf}(\Omega_1) \\ W_{of}(\Omega_1, \Omega_2) &= W_{of}(\Omega_2) - W_{of}(\Omega_1) \end{aligned} \tag{6}$$

To account for two frequency ranges, i.e., low- and high-frequency ranges, (6) has to be evaluated for both ranges and then added up.

Subsequently, a similarity transformation $T_b$ can be found from the eigenvalue problem

$$W_{cf}W_{of} = T_b \Lambda_b T_b^{-1}, \tag{7}$$

such that the (balanced) controllability and observability Gramians, $(W_{cfb})$ and $(W_{ofb})$, become equal and diagonal, i.e.,

$$W_{cfb} = W_{ofb} = \Sigma \tag{8}$$

The diagonal matrix $\Sigma$ contains the Hankel singular values, $\sigma_i$, $i = 1, \ldots, n$, known also as the second-order modes and assumed here ordered in a descending order [1], [5]. The coordinate transformation defined as $x_b = T_b^{-1}x$ provides the internally balanced system $(A_b,\ B_b,\ C_b,\ D)$:

$$\begin{aligned} \dot{x}_b &= T_b^{-1}AT_b x_b + T_b^{-1}Bu = A_b x_b + B_b u \\ y &= CT_b x_b + Du = C_b x_b + Du \end{aligned} \tag{9}$$

The frequency domain balanced system in (9) has the property that it can be reduced, via direct truncation, to the *r*th order model in (2) by preserving the first *r* largest second-order modes [1], [3]–[5]. The reduced model by FDBR is not guaranteed to be passive, so the stability of the reduced-order model cannot be guaranteed. Nonetheless, the Lyapunov equations (4) can be forced to be definite, as proposed in [20].

### B. Computational Implementation

Several balancing algorithms to compute the transformation matrix $T_b$ are described in [1] and [21]. A major computational step in these algorithms is the calculation of the singular-value decomposition (SVD) of the product of two Cholesky factors. This is especially important when calculating potentially small singular values of near-uncontrollable and near-unobservable systems [21]. In [21], an algorithm that computes the SVD of this product of matrices, without explicitly forming the product, is adopted. The complete algorithm of [21] for computing (4) and (7) is adopted for the FDBR method. Such algorithm has been compared by the authors with existing algorithms [1] for several networks. It is concluded that the algorithm from [21] provides significantly improved robustness characteristics compared to traditional algorithms.

For efficient calculation of the term *F* in (5), which is used to calculate the right-hand-side of the Lyapunov relations (4a) and (4b), we consider the structure of the matrix *A* given by the vector fitting (VF) software tool (either in complex or real form) [22]; details of the calculation of *F* are given in Appendix B.

## III. Proposed Methodology

### A. General Description

The linear part of a power electric network including one or more PECs is represented by a frequency-dependent network equivalent (FDNE) calculated for a frequency bandwidth spanning from a few Hz to a few kHz such that the switching frequencies are properly included, as depicted in Fig. 1. A major benefit of using FDNEs is substantial reduction in complexity and computational resources compared to the detailed representation for EMT simulations. Due to the wide frequency range, many resonance peaks may appear in the frequency response of the considered linear network, thus leading to a high-order approximation. The VF technique is used to obtain the rational approximation of the FDNE, referred hereinafter to as the full-order FDNE [23], and expressed in the form of

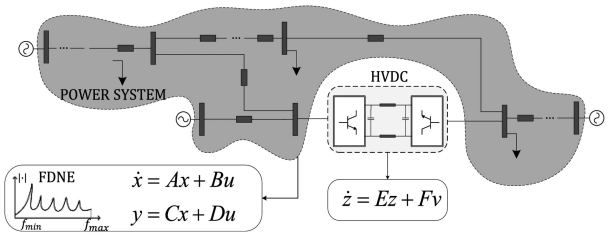


Fig. 1. Illustration of FDNE and PECs representations.

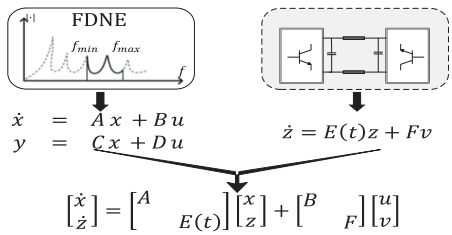


Fig. 2. Interfacing of reduced-order FDNE and the switched network part.

(1). The VF [24], Loewner Matrix (LM) [25] and Matrix Pencil Method (MPM) [26] are available techniques for the computation of rational models. All these techniques have advantages and disadvantages; for example, MPM is not able to fit functions with logarithmically-spaced sampling. VF provides high fitting accuracy (as poles follow a relocation procedure), stable poles, and passivity of the fitted system can be enforced via an in-built routine. The accuracy and robustness of VF are deemed in this paper as enough for the objective of fitting an input-admittance [27].

The full-order FDNE is then reduced via the FDBR technique, as described by (6) to (9) in Section II-B. In this paper the following three cases are considered: a) low-frequency band, b) high-frequency band, and c) combined low- and high-frequency bands. Any of these three procedures results in a reduced number of ordinary differential equations (ODE), as in (2), that closely reproduce the dynamics of the full-order model. On the other hand, the switched network subsystem is modeled in detail as a set of linear time-periodic ODEs which are interfaced to the obtained reduced-order FDNE for EMT simulation, as depicted in Fig. 2. The reduced-order models come in the form of ordinary differential equations that can be readily implemented in EMT-type simulation software tools or implemented in real-time equipment.

The FDBR-based technique is applied to a modified WSCC 9-bus test system in which an HVDC link is included. All transient waveforms presented here are obtained via the time-domain solution of the full- and reduced-order systems, as given by (1) and (2), respectively, in combination with the linear time-periodic set of ODEs corresponding to the power electronics part, and outlined in Section III-C.

### B. Test System: Linear Network Configuration

The WSCC 9-bus test system in [28] is slightly modified by connecting the HVDC system between buses $B_7$ and $B_8$, as illustrated in Fig. 3. To obtain the full-order model FDNE the following considerations are taken:

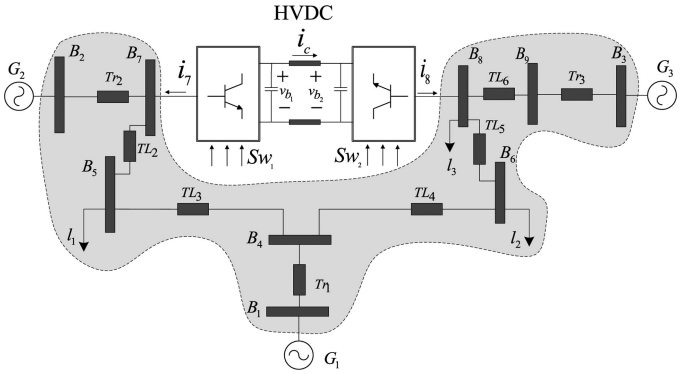


Fig. 3. WSCC 9-bus test system with the HVDC link added.

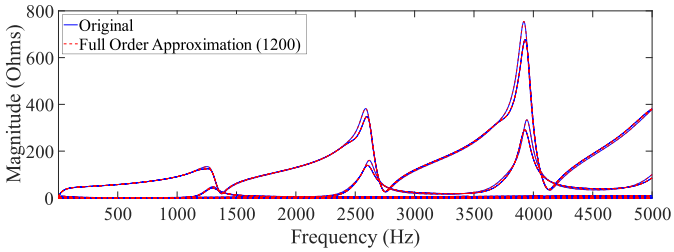


Fig. 4. Frequency response of the 5-port three-phase driving-point impedance matrix of the network in Fig. 3 and its full-order approximation.

TABLE I
TRANSMISSION LINE LENGTHS (KM) AND TRANSFORMER IMPEDANCES (PU)

| Element | $TL_2$ | $TL_3$ | $TL_4$ | $TL_5$ | $TL_6$ | $Tr_1$ | $Tr_2$ | $Tr_3$ |
|---|---|---|---|---|---|---|---|---|
| Value | 170 | 89.93 | 97.3 | 179.8 | 106 | 0.05 | 0.062 | 0.058 |

- Due to the frequency range within the scope of the studies presented in the paper which involve PECs, overhead transmission lines are modeled as a frequency-dependent distributed-parameter lines with corresponding lengths listed in Table I. The complex depth concept is utilized in their modeling and a two-port representation is considered, as in (10)–(12) [29], [30].

$$\begin{bmatrix} I_s \\ I_r \end{bmatrix} = \begin{bmatrix} Y_1 & Y_2 \\ Y_2 & Y_1 \end{bmatrix} \begin{bmatrix} V_s \\ V_r \end{bmatrix}, \tag{10}$$

where:

$$\begin{aligned} Y_1 &= Y_c \coth(\psi l), \\ Y_2 &= -Y_c \mathrm{csch}(\psi l). \end{aligned} \tag{11}$$

In (11), $l$ corresponds to the line length; $Y_c$ and $\psi$ are the characteristic admittance and propagation function of the line, respectively, related to line impedance/admittance as follows:

$$\begin{aligned} \psi &= \sqrt{ZY}, \\ Y_c &= Z^{-1}\psi. \end{aligned} \tag{12}$$

- Transformers' impedances are also listed in Table I. Loads at buses 5, 6, and 8, are arbitrarily considered here as series-connected *RL* elements with values (50, 25, 50) ohm and (50, 50, 10) mH, respectively.
- The frequency response of the 5-port driving-point impedance, seen from buses 1, 2, 3, 7, and 8, is obtained considering 1000 linear-spaced samples with frequency range from 1 Hz to 5 kHz. The elements of the resulting symmetric transfer matrix are plotted in Fig. 4.
- VF yields a passive and stable rational approximation of order 200 with a RMS error of $5.91 \times 10^{-11}$. Due to this small RMS error, the differences between the original (in continuous line) and the approximated (in dashed line) driving-point impedance elements are practically unnoticeable in Fig. 4.
- For transient analysis purposes, the three-phase current entering into buses $B_7$ and $B_8$ (named as $i_7$ and $i_8$, respectively) are considered as inputs to the FDNE and the voltages at those buses ($v_7$ and $v_8$, respectively) are considered its outputs.
- Accounting for three-phase and two inputs, the resulting dimension of the full-order state-space system, as given in (1), is of 1200.

### C. HVDC System:

The HVDC system, adopted from [31], contains two voltage-sourced converters (VSC). The time-domain model of the HVDC system is given by:

$$\begin{aligned} L_1 di_7/dt &= -Ri_7 + (Sw_1/2)v_{b1} - v_7 \\ L_2 di_8/dt &= -R_2 i_8 + (Sw_2/2)v_{b2} - v_8 \\ C_{b1} dv_{b1}/dt &= (Sw_1/2)i_7 + i_c \\ C_{b1} dv_{b2}/dt &= (Sw_2/2)i_8 - i_c \\ L_c di_c/dt &= -R_c i_c + v_{b1} - v_{b2}, \end{aligned} \tag{13}$$

where $i_7$ and $i_8$ are the currents going out of the HVDC terminals; $v_{\mathrm{b1}}$ and $v_{\mathrm{b2}}$ are the DC-link voltages and $i_{\mathrm{c}}$ its corresponding current; $v_7$ and $v_8$ correspond to the voltages at the HVDC terminals; $Sw_{_1} = 2U_{x_1} - 1$ and $Sw_2 = 2U_{x_2} - 1$ denote the switching functions provided by a sinusoidal pulse-width modulation (PWM) scheme using a switching frequency of 1.5 kHz.

## IV. NUMERICAL RESULTS

To assess the performance and accuracy of the proposed methodology, the network of Fig. 3 is considered in this Section. The frequency bandwidths entered into FDBR method are assumed as

- Low-frequency (LF) band, from 1 Hz to 100 Hz.
- High-frequency (HF) band, from 3 kHz to 5 kHz.
- Two bands (2B), from 1 Hz to 100 Hz and from 1 kHz to 5 kHz.

Later in this Section, transient simulations are carried out using the trapezoidal rule of integration method with step size of 10 $\mu$s. It is shown that both LF and HF ranges are necessary to obtain an accurate representation of the interfacing between the FDNE and switched network subsystem.

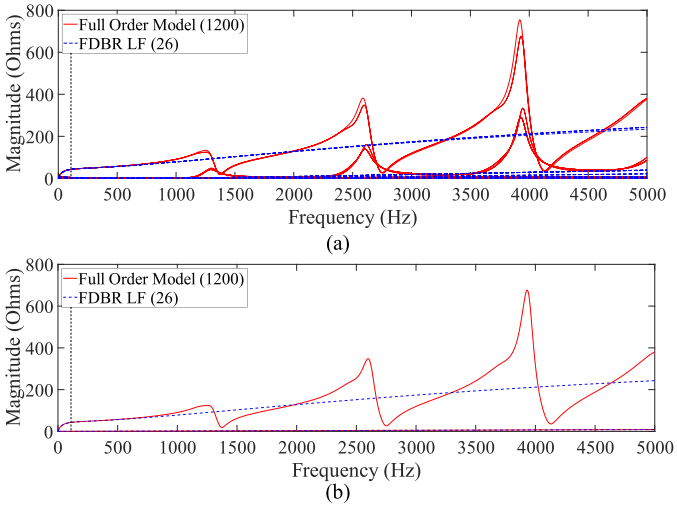


Fig. 5. (a) LF reduced-order approximation of 5-port three-phase driving-point impedance matrix (all elements) and (b) Elements (1, 1) and (6, 6).

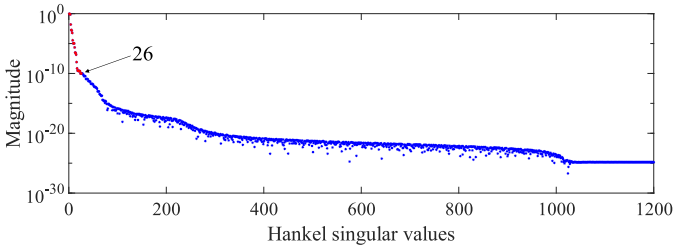


Fig. 6. Hankel singular values of balanced system applying FDBR in LF range.

### A. MOR Using FDBR: LF Band

Figure 5 shows the frequency response of the reduced-order model provided by FDBR in the LF range, presenting only elements (1, 1) and (6, 6) of the driving-point impedance matrix in Fig. 5(b) for visibility purposes. The obtained model is of order 26 which is about 2% of the full-order model (1200th order). This reduced-order model is chosen based on the Hankel values provided by FDBR, presented in Fig. 6, with a magnitude threshold of $10^{-10}$. The high accuracy of approximation in the pre-specified low-frequency range can be observed from Fig. 5. On the contrary, HF error of approximation is noticeable; this can lead to inaccurate fast dynamics reproduction by the reduced-order model.

### B. MOR Using FDBR: HF Band

Figure 7 presents the frequency response of the reduced-order model provided by FDBR in the HF range. The reduced-order model is of order 72 which is about 6% of the full-order model. Also, a magnitude threshold of $10^{-10}$ is used to choose dominant Hankel values, presented in Fig. 8. Figure 7 shows strong agreement between full- and reduced-order approximations in the pre-specified high-frequency range. For this case study, an accurate HF interaction is expected between FDNE and PECs dynamics.

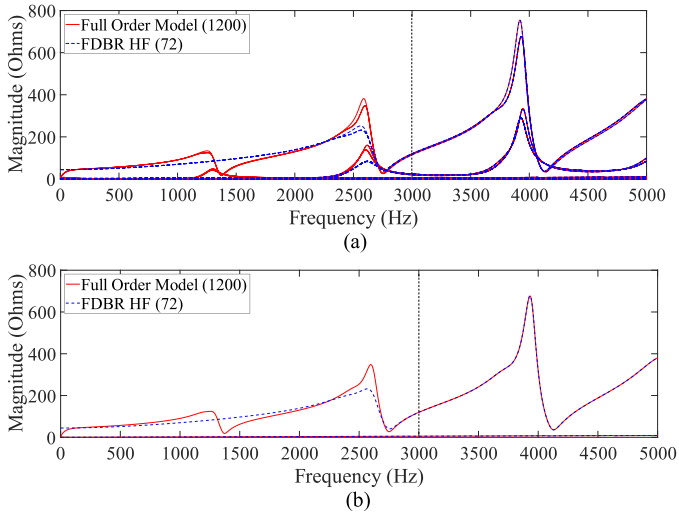


Fig. 7. HF reduced-order approximation of 5-port three-phase driving-point impedance matrix (a) All elements and (b) Elements (1, 1) and (6, 6).

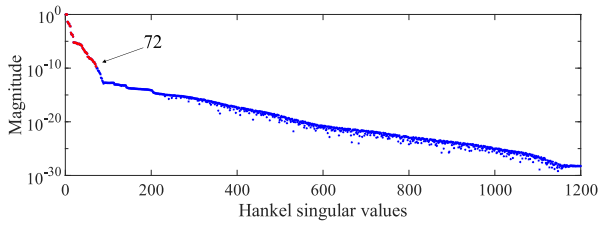


Fig. 8. Hankel singular values of balanced system applying FDBR in HF range.

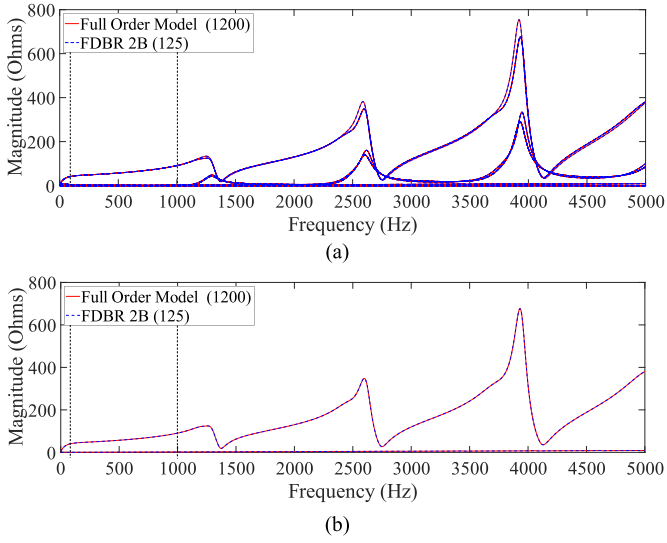


Fig. 9. Two-band approximation of 5-port three-phase driving-point impedance matrix (a) All elements and (b) Elements (1, 1) and (6, 6).

### C. MOR Using FDBR: LF and HF Bands

Figure 9 presents the frequency response of the reduced-order model provided by FDBR when specifying both low- and high-frequency ranges for the reduction process. Using a magnitude threshold of $10^{-10}$ to choose dominant Hankel

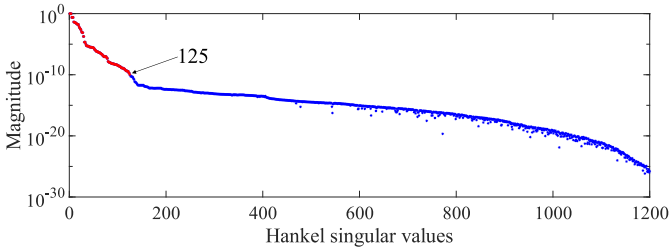


Fig. 10. Hankel singular values of two-band reduced balanced system.

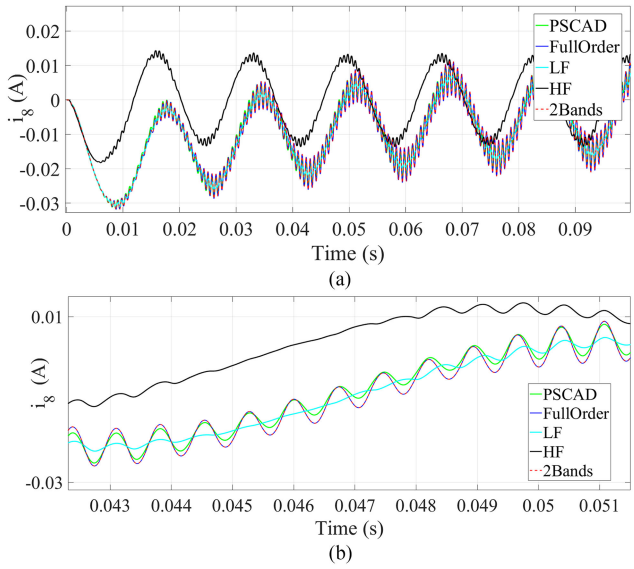


Fig. 11. (a) Transient current $i_8$, phase-$a$, given by full-order (1200th) and by FDBR reduced-order models (LF, HF, and two-band). (b) Zoom-in.

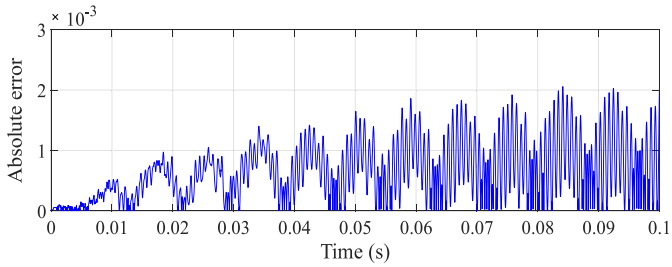


Fig. 12. Absolute error for current $i_8$, phase-$a$, between the 1200th-order system and PSCAD/EMTDC.

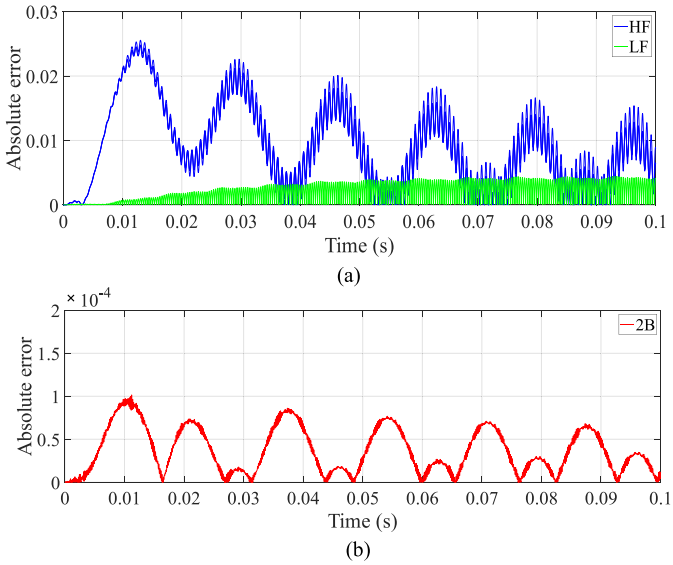


Fig. 13. Absolute error for current $i_8$, phase-$a$, (a) between LF and HF reduced-order models and 1200th order and (b) between two-band reduced-order system and 1200th order.

values, presented in Fig. 10, yields a reduced-order model of order 125 which represents about 10.4% of the full-order model. Figure 9 shows that a strong agreement exists between full- and two-band approximations.

### *D. Transient Simulation Case Study 1*

The three reduced-order models obtained via FDBR, i.e., LH, HF, and two-band, are verified and compared against the full-order model by using transient simulation. Also, for verification purposes, the transient waveforms by the power systems computer aided (PSCAD/EMTDC) software tool are included in some figures. For simplicity of exposition, the transient scenario is as follows. The network is energized at $t = 0$ s via unit sinusoidal input voltages for all generators $G_1$, $G_2$, and $G_3$. Initial conditions are assumed zero. Fig. 11 presents the transient waveforms for current entering bus $B_8$, phase-$a$ (similar results are obtained for phases $b$ and $c$). The results in Fig. 11 are obtained with full-order and the three outlined reduced-order models. Also, the transient waveform given by PSCAD/EMTDC is included in Fig. 11. It is noted that in the close-up of Fig. 11(b) the waveforms by full-order and two-band reduced-order model superimpose and their difference is unnoticeable. Fig. 11(b) shows that the LF approximation averages the frequencies associated with the switching frequency. On the other hand, Fig. 11(a) shows that the HF approximation agrees with the full-order model and PSCAD simulations; however, it deviates when heading to stationary state. Fig. 12 presents the absolute error between the full-order model and PSCAD/EMTDC. This error can be attributed to the different assumptions that PSCAD/EMTDC involves, such as interpolation, losses in switching devices, among others. Fig. 13 presents the absolute error along the simulation time-window between the three reduced-order models, and the full-order model.

Although LF band reduction should exhibit smaller error at the end of the simulation window, the opposite happens. This is due to the *averaging* effect as the stationary state develops, see Fig. 11(b). HF dynamics from switching devices remain along the simulation time-window. At the end of the time-window, such HF oscillations dominate over the stationary state.

As for the HF band reduction, the error is small for a very short time and then increases as steady-state develops, as expected, and confirmed in Figs. 11 and 13(a). As seen in Fig. 7, the HF reduced-order model deviates from the full-order model at

TABLE II
CPU TIMES FOR FULL- AND REDUCED-ORDER MODELS, CASE STUDY 1

| Model | CPU time (s) | RMS Error between Full-order & PSCAD | RMS Error between Full- and reduced-order models |
|---|---|---|---|
| PSCAD | 2.8 | - | - |
| Full-order | 1193.5 | 0.0013 | - |
| FDBR LF | 3.86 | - | 0.0027 |
| FDBR HF | 6.17 | - | 0.0093 |
| FDBR 2B | 6.57 | - | $4.053\times10^{-5}$ |

low frequencies; thus, even though HF ripple is exhibited at the end of the simulation in Fig. 11, the magnitude of the transient waveform results different than that given by the full-order model.

The smallest error is achieved by the two-band reduced model. It is remarkable that such error is kept almost constant along the simulation time-window, Fig. 13(b), showing effectiveness in the reproduction of low- and high-frequency dynamics.

The CPU-times and RMS-errors for this case study are presented in Table II. Both full- and reduced-order models have been programmed under Matlab environment and simulated using a computer with an Intel Core i7-4700HQ CPU @ 2.40 GHz and 8 GB RAM. Table II shows that substantial computational savings are achieved by the three reduced-order models with respect to the full-order model. Specifically, the CPU-time by the two-band reduced-order model is an advantage for multiple simulations when designing control systems, since the system modes that represent important dynamics are considered accurately.

### E. Transient Simulation Case Study 2

Further verification of the proposed methodology is presented in this section via a second case study. The system in Fig. 3 is considered also for this case study. The transient scenario consists of the starting-up and application of a three-phase fault at $t = 0.05$ s at the HVDC right-hand-side terminal via a low resistance of 0.001 ohm. The two-band reduced-order model is compared with the full-order model and the PSCAD/EMTDC. Based on the full-order (order 1200) system of Fig. 4, the frequency ranges for the two-band reduced system are again from 1 Hz to 100 Hz and from 3 kHz to 5 kHz. The two-band reduced-order model is obtained via FDBR and results in an order of 125. The transient waveforms for voltage $v_8$, phase $a$, given by full-order, two-band reduced-order, and PSCAD/EMTDC, are presented in Fig. 14. The RMS error between full- and two-band reduced-order is of $2.31 \times 10^{-4}$. The CPU-times are 1193 s, 6.57, and 2.9 s, by full-order, two-band reduced-order, and PSCAD/EMTDC, respectively.

## V. APPROXIMATION AND TIME-DOMAIN ERRORS: FURTHER ANALYSIS

Classical BR provides approximation $(e_r)$ and closeness $(E_r)$ errors, as given by (14) and (15), respectively, [5]. On the other hand, FDBR tends to keep the error bounds within the frequency bandwidth of approximation. This section provides

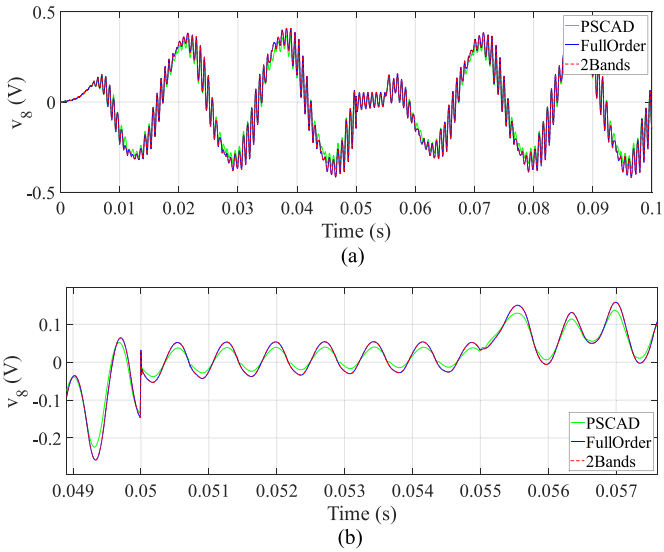


Fig. 14. (a) Transient voltage $v_8$, phase-$a$, given by full-order (1200th) and two-band reduced-order models. (b) Zoom-in.

TABLE III
ERRORS FOR DIFFERENT ORDERS OF REDUCTION, CASE STUDY 1

| $r$ | $E_r$ | $e_r$ |
|---|---|---|
| 70 | $0.12\times10^{-6}$ | 0.0151 |
| 80 | $0.01\times10^{-6}$ | 0.0113 |
| 110 | $0.008\times10^{-6}$ | 0.0097 |
| 125 | $0.001\times10^{-6}$ | **0.0035** |

TABLE IV
ERRORS FOR DIFFERENT FREQUENCY BANDWIDTHS, CASE STUDY 1

| LF band \ HF band | 1 kHz – 2 kHz | 1kHz – 3 kHz | 1 kHz – 5 kHz |
|---|---|---|---|
| 1 Hz – 50 Hz | 0.0201 | 0.0215 | 0.55 |
| 1 Hz – 70 Hz | 0.0193 | 0.0211 | 0.3482 |
| 1 Hz – 100 Hz | 0.0183 | 0.0205 | **0.0035** |

further numerical insight of approximation and time-domain errors when reducing in two frequency ranges. Also, numerical results on order reduction are presented.

$$e_r = \sqrt{\sum_{k=1}^{N} [f_n(k) - f_r(k)]^2} \Big/ \sqrt{\sum_{k=1}^{N} [f_n(k)]^2}, \tag{14}$$

$$E_r = \sqrt{\sum_{i=r+1}^{n} \sigma_i^2} \Big/ \sqrt{\sum_{i=1}^{r} \sigma_i^2} \tag{15}$$

where $f_n$ and $f_r$ represent the time-domain transient waveforms of the full- and reduced-order systems, respectively, and $N$ denotes the number of time-domain samples.

Table III lists the closeness $E_r$ and time-domain relative error $e_r$ for different model orders, based on the Hankel values in Fig. 10, as given between full-order and two-band reduced-order model for case study 1 presented in Subsection IV-C.

Table IV lists $e_r$ when approximating in different two-band frequency ranges, noting that the best approximation is obtained

for the ranges from 1 Hz to 100 Hz and from 1 kHz to 5 kHz (bold type in Table IV). This reinforces our proposal of two-band frequency MOR.

## VI. Conclusions

A MOR methodology based on the FDBR technique is presented in the paper for EMT simulation of power networks involving PECs. It is shown that excellent agreement of dynamics behavior is achieved by applying FDBR in two frequency bands at a time, i.e., low- and high-frequency ranges. The utilized criteria for the two frequency bands are (i) frequencies involving fundamental power frequency and (ii) frequencies enclosing switching frequency of PECs. The proposed methodology is verified via a test network including a transmission subsystem and an HVDC link. The time-domain dynamics of the full- and two-band reduced-order model strongly agree, and computational savings are achieved by the latter model.

## Appendix A

The classical time-domain BR theory is well known; this section discusses only the basic relationships [5]. The controllability $W_c$ and observability $W_o$ Gramians of the full-order state-space model (1) are given in time-domain by

$$W_c = \int_0^\infty e^{At} B B^T e^{A^T t} dt, \tag{16a}$$

$$W_o = \int_0^\infty e^{A^T t} C^T C e^{At} dt \tag{16b}$$

Both Gramians in (16) satisfy the Lyapunov relations:

$$A W_c + W_c A^T = -B B^T, \tag{17a}$$

$$A^T W_o + W_o A = -C^T C \tag{17b}$$

A similarity transformation $T_b$ can be found from the eigenvalue problem:

$$W_c W_o = T_b \Lambda_b T_b^{-1}, \tag{18}$$

such that the controllability and observability Gramians are equal and diagonal, i.e.,

$$W_{cb} = W_{ob} = \Sigma \tag{19}$$

The new coordinate system, given by (18) allows obtaining an internally balanced system $(A_b,\ B_b,\ C_b)$ as in (9). Truncation is applied to $(A_b,\ B_b,\ C_b)$ to obtain $(A_r,\ B_r,\ C_r)$, as in (2). Some algorithms to compute (18) can be found in [1], [14]. It is shown that the error in the transfer function of the reduced model is bounded by [5]

$$\|H_n(s) - H_r(s)\|_\infty \leq 2 \sum_{i=r+1}^{n} \sigma_i \tag{20}$$

## Appendix B

Considering that the fitted system given by VF is converted into a real-valued system via a similarity transformation, matrix $F$ of (5) can be directly obtained in two parts, each one corresponding to real and complex poles. Since only complex poles of $A$ are modified by the similarity transformation, each $k$th complex pair of poles of the diagonal matrix $A$ become a sub-matrix of the form

$$\begin{bmatrix} a' & a'' \\ -a'' & a' \end{bmatrix}, \tag{21}$$

with:

$$a_k = a' + j a'' \tag{22}$$

The $p$ elements of matrix $F$ corresponding to the real poles can be directly evaluated as follows:

$$F_{i,i} = -\ln(\omega + j a_i)\big|_{\omega_1}^{\omega_2}, \quad i = 1, 2, \ldots, p, \tag{23}$$

while the elements of $F$ corresponding to the $2 \times 2$ sub-matrices, as in (21), are given by

$$F_{k,k+1} = -j \arctan\left(\frac{j\omega - a'}{a''}\right)\Bigg|_{\omega_1}^{\omega_2} = -F_{k+1,k}, \tag{24a}$$

$$F_{k,k} = F_{k+1,k+1} = \frac{1}{2j} \ln\left(a'^2 + a''^2 - \omega^2 - 2j\omega a''\right)\Bigg|_{\omega_1}^{\omega_2}. \tag{24b}$$

## References


[1] A.C. Antoulas, *Approximation of Large-Scale Dynamical Systems, series on Advances in Design and Control*. Philadelphia, PA, USA: SIAM, 2005.

[2] S. R. Sanders, J. M. Noworolski, X. Z. Liu, and G. C. Verghese, "Generalized averaging method for power conversion circuits," *IEEE Trans. Power Electron.*, vol. 6, no. 2, pp. 251–259, Apr. 1991.

[3] P. Benner, V. Mehrmann, and D.C. Sorensen, "Dimension reduction of large-scale systems," *Lecture Notes in Computational Science and Engineering*, vol. 45. Berlin, Germany: Springer, Jun. 2005.

[4] W.H.A. Schilders, H. A. van der Vorst, and J. Rommes, *Model Order Reduction: Theory, Research Aspects, and Applications*, vol. 13. Berlin, Germany: Springer, 2008.

[5] B. Moore, "Principal component analysis in linear systems: Controllability, observability, and model reduction," *IEEE Trans. Autom. Control*, vol. AC-26, no. 1, pp. 17–32, Feb. 1981.

[6] J. Harrison, "A frequency-domain approach to frequency-weighted balanced realization," *IEEE Trans. Circuits Syst. I, Fundam. Theory Appl.*, vol. 50, no. 5, pp. 655–662, May 2003.

[7] M. Mattingly, E.A. Bailey, A.W. Dutton, R.B. Roemer, and S. Devasia, "Reduced-order modeling for hyperthermia: An extended balanced-realization-based approach," *IEEE Trans. Biomed. Eng.*, vol. 45, no. 9, pp. 1154–1162, Sep.1998.

[8] F. Cingoz, A. Bidram, and A. Davoudi, "Reduced order, high-fidelity modeling of energy storage units in vehicular power systems," in *Proc. IEEE Vehicle Power Propulsion Conf.*, 2011, pp. 1–6.

[9] M. Bettayeb and U. M. Al-Saggaf, "Practical model reduction techniques for power systems," *Elect. Power Syst. Res.*, vol. 25, no. 3, pp. 169–176, 1992.

[10] S. D. Đukić and A. T. Sarić, "Dynamic model reduction: An overview of available techniques with application to power systems," *Serbian J. Elect. Eng.*, vol. 9, no. 2, pp. 131–169, 2012.

[11] M. K. Vakilzadeh, S. Rahrovani, and T. Abrahamsson, "Modal reduction based on accurate input-output relation preservation," *Topics Modal Anal.*, vol. 7, pp. 333–342, 2014.

[12] Z. Zhu, G. Geng, and Q. Jiang, "Power system dynamic model reduction based on extended Krylov subspace method," *IEEE Trans. Power Syst .*, vol. 31, no. 6, pp. 4483–4494, Nov. 2016.

[13] X. Cheng and J. M. A. Scherpen, "Clustering approach to model order reduction of power networks with distributed controllers," *Adv. Comput. Math.*, vol. 44, no. 6, pp. 1917–1939, 2018.

[14] A. Ramirez *et al.*, "Application of balanced realizations for model-order reduction of dynamic power system equivalents," *IEEE Trans. Power Del.*, vol. 31, no. 5, pp. 2304–2312, Oct. 2016.

[15] G. Troullinos and J. F. Dorsey, "Application of balanced realizations to power system equivalents," *IEEE Trans. Autom. Control*, vol. AC-30, no. 4, pp. 414–416, Apr. 1985.
[16] A. Lopez and A.R. Messina, "An optimal modal approximation method for model reduction of linear power system models," *Int. J. Elect. Power Energy Syst.*, vol. 44, no. 1, pp. 293–300, Jan. 2013.
[17] A. Adib, B. Mirafzal, X. Wang, and F. Blaabjerg, "On stability of voltage source inverters in weak grids," *IEEE Access*, vol. 6, pp. 4427–4439, 2018.
[18] P. Vorobev, P. Huang, M. Al Hosani, J. L. Kirtley, and K. Turitsyn, "High-fidelity model order reduction for microgrids stability assessment," *IEEE Trans. Power Syst.*, vol. 33, no. 1, pp. 874–887, Jan. 2018.
[19] A. Zilouchian, P.K. Agaee, and K. Nickravesh, "Model reduction of large scaled systems via frequency-domain balanced structures," in *Proc. IEEE Proc. Amer. Control Conf.*, Jun. 1997, vol. 6, pp. 3873–3876.
[20] J.R. Phillips, L. Daniel, and L.M. Silveira, "Guaranteed passive balancing transformations for model order reduction," *IEEE Trans. Comput.-Aided Design Integr. Circuits Syst.*, vol. 22, no. 8, pp. 1027–1041, Aug. 2003.
[21] A. J. Laub, M.T. Heath, C.C. Paige, and R.C. Ward, "Computation of system balancing transformations and other applications of simultaneous diagonalization algorithms," *IEEE Trans. Autom. Control*, vol. AC-32, no. 2, pp. 115–122, Feb. 1987.
[22] A. Semlyen and B. Gustavsen, "A half-size singularity test matrix for fast and reliable passivity assessment of rational models," *IEEE Trans. Power Del.*, vol. 24, no. 1, pp. 345–351, Jan. 2009.
[23] U. D. Annakkage *et al.*, "Dynamic system equivalents: A survey of available techniques," *IEEE Trans. Power Del.*, vol. 27, no. 1, pp. 411–420, Jan. 2012.
[24] B. Gustavsen and A. Semlyen, "Rational approximation of frequency domain responses by vector fitting," *IEEE Trans. Power Del.*, vol. 14, no. 3, pp. 1052–1061, Jul. 1999.
[25] S. Lefteriu and A. C. Antoulas, "A new approach to modeling multiport systems from frequency-domain data," *IEEE Trans. Comput.-Aided Des. Integr. Circuits Syst.*, vol. 29, no. 1, pp. 14–27, Jan. 2010.
[26] K. Sheshyekani, H. R. Karami, P. Dehkhoda, M. Paolone, and F. Rachidi, "Application of the matrix pencil method to rational fitting of frequency-domain responses," *IEEE Trans. Power Del.*, vol. 27, no. 4, pp. 2399–2408, Oct. 2012.
[27] J. Morales, E. Medina, J. Mahseredjian, A. Ramirez, K. Sheshyekani, and I. Kocar, "Frequency-domain fitting techniques: A review," *IEEE Trans. Power Del.*, to be published, doi: 10.1109/TPWRD.2019.2932395.
[28] Illinois Center for a Smarter Electric Grid. 2013. [Online]. Available: http://publish.illinois.edu/smartergrid/
[29] L. M. Wedepohl and S. E. T. Mohamed, "Multiconductor transmission lines. Theory of natural modes and Fourier integral applied to transient analysis," in *Proc. Inst. Elect. Eng.*, Sep. 1969, vol. 116, no. 9, pp. 1553–1563.
[30] A. Deri, G. Tevan, A. Semlyen, and A. Castanheira, "The complex ground return plane: A simplified model for homogeneous and multilayer earth return," *IEEE Trans. Power App. Syst.*, vol. PAS-100, no. 8, pp. 3686–3693, Aug. 1981.
[31] A. Yazdani and R. Iravani, "Dynamic model and control of the NPC-based back-to-back HVDC system," *IEEE Trans. Power Del.*, vol. 21, no. 1, pp. 414–424, Jan. 2006.

**Carlos A. Ruiz-Zea** (S'19) received the B.Sc. degree in control engineering from the Universidad Nacional de Colombia, Bogotá, Colombia, in 2016, and the M.Sc. degree in electrical engineering from the Center for Research and Advanced Studies of Mexico, Guadalajara, Mexico, in 2018, where he is currently working toward the Ph.D. degree. His research interests include transient analysis and control design of power systems with embedded power electronic converters.

**Edgar Medina** (S'15) received the B.Sc. degree in electrical engineering from Universidad Autonoma de San Luis Potosi, San Luis Potosi, Mexico, in 2012, and the M.Sc. degree in electrical engineering from the Center for Research and Advanced Studies of Mexico, Guadalajara, Mexico, in 2015, where he is currently working toward the Ph.D. degree. He was a Visitor Student with the Polytechnique of Montreal, Montreal, QC, Canada. His research interests include transient analysis of power systems and simulation of electromagnetic transients.

**Abner Ramirez** (SM'07) received the B.Sc. and M.A.Sc. degrees from the University of Guanajuato, Guanajuato, Mexico, in 1996 and 1998, respectively, and the Ph.D. degree from the Center for Research and Advanced Studies of Mexico (CINVESTAV), Guadalajara, Mexico, in 2001. From November 2001 to January 2005, he was a Postdoctoral Fellow with the Department of Electrical and Computer Engineering, University of Toronto, Toronto, ON, Canada. He is currently a Faculty Member with CINVESTAV. His research interests include electromagnetic transient analysis in power systems and numerical analysis of electromagnetic fields. He is a member of the Mexican Association of Professionals and Entrepreneurs.

**Ali Mehrizi-Sani** (S'0–M'12–SM'15) received the Ph.D. degree from the University of Toronto, Toronto, ON, Canada, in electrical engineering, in 2011. He is currently an Associate Professor with Virginia Tech, Blacksburg, VA, USA. He previously was an Associate Professor with Washington State University, Pullman, WA, USA, and a Visiting Professor at Graz University of Technology (TU Graz), Graz, Austria. His areas of interest include power system applications of power electronics and integration of renewable energy resources. He is an Editor of the IEEE TRANSACTIONS ON POWER SYSTEMS, the IEEE TRANSACTIONS ON ENERGY CONVERSION, and the IEEE POWER ENGINEERING LETTERS. He is the recipient of 2018 IEEE PES Outstanding Young Engineer Award, 2018 ASEE PNW Outstanding Teaching Award, 2017 IEEE Mac E. Van Valkenburg Early Career Teaching Award, 2017 WSU EECS Early Career Excellence in Research, 2016 WSU VCEA Reid Miller Excellence in Teaching Award, 2011 NSERC Postdoctoral Fellowship, and 2007 Dennis Woodford Prize for his M.Sc. thesis. From 2007 to 2011, he was a Connaught Scholar at the University of Toronto.

**Jose de Jesus Chavez** (S'07–M'10) received the M.A.Sc. and Ph.D. degrees from the Center for Research and Advanced Studies of Mexico, Guadalajara, Mexico, in 2006 and 2009, respectively. From 2010 to 2016, he was a Professor with the National Technological Institute of Mexico Campus Morelia. Since 2016, he is with the Intelligent Electrical Power Grids, Delft University of Technology, Delft, the Netherlands. His interests are electromagnetic transient analysis in power systems, real-time simulation, wide and local area protection, and HiL.

**Ali Davoudi** (S'04–M'11–SM'15) received the Ph.D. in electrical and computer engineering from the University of Illinois, Urbana-Champaign, IL, USA, in 2010. He is currently an Associate Professor with the Electrical Engineering Department, University of Texas, Arlington, TX, USA. He is an Associate Editor for the IEEE TRANSACTIONS ON POWER ELECTRONICS, the IEEE TRANSACTIONS ON TRANSPORTATION ELECTRIFICATION, the IEEE TRANSACTIONS ON ENERGY CONVERSION, and the IEEE POWER LETTERS. More recently, he has received the Best Paper Award from 2015 IEEE International Symposium on Resilient Control Systems, 2014–2015 Best Paper Award from the IEEE Transactions on Energy Conversion, 2016 Prize Paper Award from the IEEE Power and Energy Society, 2017 IEEE Richard M. Bass Outstanding Young Power Electronics Engineer Award, and 2017–2018 Best Paper Award from the IEEE TRANSACTIONS ON ENERGY CONVERSION.

**Mohamed Abdel-Rahman** (SM'07) was born in 1973, in Cairo, Egypt. He received the B.Sc. degree from Ain Shams University, Cairo, Egypt, in 1995, the M.A.Sc. and Ph.D. degrees from the University of Toronto, Toronto, ON, Canada, in 1998 and 2001,respectively, all in electrical engineering. He is currently a Professor with the Department of Electrical Power and Machines Engineering Department, Faculty of Engineering, Ain Shams University. His research interests are power system modeling, and simulation and integration of large-scale renewable energy resources into electrical grids.